RSC Advances

ROYAL SOCIETY OF CHEMISTRY

www.rsc.org/advances

Two-dimensional electrospun nanofibrous membranes for promoting random skin flap survival

Xiaoming Sun[1a], Reila Zheng[1b], Liying Cheng[a], Xin Zhao[b], Rong Jin[a], Lu Zhang[a], Ying Zhang[a*], Yuguang Zhang[a*], Wenguo Cui[b*]

[a] Department of Plastic and Reconstructive Surgery, Ninth People's Hospital affilicated to Medical School of Shanghai Jiao Tong University, 639 Zhi Zao Ju Road, Shanghai 200011, P.R. China.

[b] Department of Orthopedics, The First Affiliated Hospital of Soochow University, Orthopedic Institute, Soochow University, 708 Renmin Road, Suzhou, Jiangsu 215006, P. R. China.

[1] The two authors contributed equally.

* Corresponding authors:

Fax/Tel: +86-512-67781420, +86-21-63089562.

E-mail: wgcui80@hotmail.com (WG Cui); zyinghh@163.com (Y Zhang); zhangygresearch@126.com (YG Zhang);

Abstract

Random skin flaps are widely used for repairing and reconstructing tissue defects and local tissue loss, and efforts to improve the survival of random skin flaps are continually being developed. Biomaterial scaffolds provide a microstructure for cell growth. However, the conventional three-dimensional structure can cause large foreign body reactions in the local subcutaneous tissue leading to fibrosis in order to block the blood perfusion of the skin flap. In this study, the effect of two-dimensional electrospun nanofibrous membranes on random skin flaps survival was investigated. Both typical nanofibrous membranes of synthetic (poly (L-lactide)) and natural (gelatin) materials were fabricated and analyzed using scanning electron microscopy, uniaxial tensile and water contact angle measurements. Both kinds of membranes maintained stable fibrous structures, but the natural fiber showed a better adhesion and viability for human dermal fibroblasts (HDFs) and human umbilical vein endothelial cells (HUVECs) compared to synthetic fibers. *In vivo* experiments showed that natural electrospun nanofibrous membranes had faster degradation, better revascularization, and caused less inflammation, leading to an improved random skin flap survival. Therefore, electrospun fibrous membranes made of natural materials are more advantageous for random skin flap survival compared to the synthetic ones, and may be used as carrier implantation materials for improving skin flap survival rate.

Key words: random skin flap, regeneration, electrospinning, two-dimensional, nanofibrous membranes, poly (L-lactide), gelatin

Introduction

Random skin flap is an approach to repair local defects widely used in clinical practice.[1] However, partial or complete failure of random skin flaps surgery remains a significant problem in plastic and reconstructive surgery because of risk factors such as elderly patients in their elderly age, bad habits such as alcohol or tobacco use, local and systemic disorders such as Renault's syndrome or diabetes mellitus.[2-4] Until recently, repeated changing of the wound dressing or skin grafts were the only procedures to treat skin flap necrosis, performed only after necrosis occurs. Up to now, the surgical delay procedure has been used as the only proven technique to improve skin flap survival.[5-6] Recently, methods to reduce skin flap necrosis by early intervention have become a popular research topic.

Currently, the main methods to prevent skin flap necrosis include injection of drugs (e.g., aminoguanidine),[7] growth factors (e.g., VEGF),[8] and stem cells (e.g., mesenchymal stem cells).[9] However, frequent injections may cause pain for patients, and growth factors or drugs have the disadvantage of a short half-life, low efficiency by local application, and significant side effects by systemic application. In addition, local injections of stem cells can easily lead to uneven distribution in the subcutaneous tissue, which may not only affect stem cell survival and cell activity, but also cause local tissue overgrowth leading to local fibrosis. Utilizing the knowledge of the mechanism of action of growth factors, drugs, and stem cells to enhance the skin flap survival rate, may be useful to optimize their distribution in the tissues to maximize in the skin flap biological activity.

Biodegradable biomaterial scaffolds consist of biodegradable medical materials that provide microenvironments for cell growth.[10,11] However, the conventional three-dimensional (3D) structure of the biomaterial scaffolds, which could cause a significant foreign body reaction in the local subcutaneous tissue leading to fibrosis to block the blood perfusion of the skin flap. Electrospun nanofibrous membrane is a porous two-dimensional (2D) nano-material composed of nanofibers, which maintains cell growth and nutrient exchange.[12,13] Moreover, a 2D membrane would not result in serious foreign body reactions because of its small volume. As a result, the 2D electrospun nanofibrous membrane implanted under the random skin flap, might fully utilize their characteristics of biological materials properties to improve the success rate of the skin flap technique.

The materials constituting the biodegradable electrospun nanofibrous membranes can be divided into natural and synthetic biomaterials, both possessing a very good nanometer fiber structure after electrospinning.[14,15] However, these two biomaterials would influence in a different manner the survival rate of skin flap due to the different membrane materials components. In this study, natural polymer gelatin and synthetic polymers poly (L-lactide), which are the most conventional materials used in tissue repair, were used to successfully prepare electrospunning gelatin and poly (L-lactide) nanofibrous membranes. Next, we analyzed the influence of these two nanofibrous membranes on the random skin flaps performance (Scheme 1). Therefore, the aim of this study was to characterize the morphology, surface wettability, and influence on human dermal fibroblasts (HDFs) and human umbilical vein endothelial cells (HUVECs) survival *in vitro*, and investigated their influence on the random skin flap survival *in*

vivo in a rat model.

Materials and methods

Materials

Poly(L-lactide) (PLLA, Mw=50 kDa, Mw/Mn=2.05) was prepared by bulk ring-opening polymerization of lactide using stannous chloride as an initiator (Jinan Daigang Biomaterial Co, Ltd, Jinan, People's Republic of China).[16] Gelatin (porcine skin, type B powder) was purchased from Sigma (St. Louis, MO). All other chemicals and solvents were reagent grade and purchased from Guoyao Regents Company (Shanghai, People's Republic of China).

Preparation of electrospun fibrous membranes

The electrospinning process was performed as described elsewhere.[17] To prepare the gelatin electrospun solution, 2.0 g gelatin was totally dissolved into 18 ml hexafluoroisopropanol (HFP). To prepare the PLLA electrospun solution, 2.0 g PLLA was totally dissolved into 8.0 ml dichloromethane and 4.0 ml dimethylformamide. The electrospinning apparatus was equipped with a high-voltage statitron (Tianjing High Voltage Power Supply Co., Tianjing, China) of maximal voltage of 30 kV. The electrospun solution was added in a 5 ml syringe attached to a circular-shaped metal syringe needle as the nozzle. An oblong counter electrode was located approximately 15 cm from the capillary tip. The flow rate of the polymer solution was controlled by a precision pump to maintain a steady flow from the capillary outlet. All the electrospun fibrous mats were vacuum-dried at room temperature for 2 days to completely remove any solvent residue. The gelatin electrospun fibers were further stored in ethanol with

2% glutaraldehyde for cross-linking overnight, then the cross-linked gelatin fibers were washed with PBS and used in the cell culture and animal experiments.

Characterization of electrospun fibers

The thickness of the fibrous scaffolds was measured with a micrometer, and their apparent density and porosity were calculated according to previous methods.[18] The morphology of fibrous scaffolds was observed using scanning electron microscopy (SEM, FEI Quanta 250, Netherlands) after sputtering Pt/Pd metal for 90 seconds onto the sample. At least five images were taken for each scaffold sample and scaffolds' fiber diameter was measured from SEM images.[18]

For mechanical property tests, dry electrospun fibrous scaffolds were punched into small strips (70.0× 7.0×0.6 mm^3). Uniaxial tensile tests were performed using an all purpose mechanical testing machine (Instron 5567, Norwood, MA) and the fibrous scaffolds' stress-strain curves were constructed from the load deformation curves recorded at a stretching speed of 0.5 mm/s (n=5). From the stress-strain curves, the scaffolds' Young's modulus, tensile strength, and elongation at break were obtained.

Electrospun scaffolds' surface wettability was detected by a water contact angle (WCA) method at room temperature. The WCAs of different fibrous scaffolds were measured with a Kruss GmbH DSA 100 Mk 2 goniometer (Hamburg, Germany) followed by image processing of sessile drop with DSA 1.8 software.

***In vitro* cell culture on membranes**

To examine the cell behavior on the electrospun nanofibrous membranes, HDFs were isolated from human hypertrophic scars provided by the Department of Plastic and

Reconstructive Surgery, Ninth People's Hospital Affiliated to Medical School of Shanghai Jiao Tong University (Shanghai, China). HDFs were used at passage 2 to 4. HUVECs were kindly provided by the Tissue Engineering Laboratories. Ninth People's Hospital Affiliated to Medical School of Shanghai Jiao Tong University (Shanghai, China) and were used at passage 3. All cells were cultured in Dulbecco's Modified Eagle Medium (DMEM, Gibco, Grand Island, NY, USA) supplemented with 10% fetal bovine serum (FBS; Gibco), penicillin (100 units per ml), and streptomycin (100 μg ml^{-1}) (Sigma). The cells were maintained in a humidified incubator at 37°C with 5% CO_2. Culture media were replaced every three days.

After sterilization, the electrospun fibrous membranes were cut into disks with a diameter of 24 mm, which was slightly larger than the 12-well culture plate diameter (Costar, Corning, NY, USA). Next, the membranes were pre-wet with cell culture medium for 4h. 100μl of HDF suspension (8×10^5 cells per ml) and 100μl of HUVECs suspension (9×10^5 cells per ml) were separately seeded on the surfaces of the membranes and placed in the 12-well culture plates (Costar, Corning, NY, USA). The plates were incubated at 37°C with 5% CO_2 for 4 h before 1 ml of culture medium was added into each well. The culture medium was changed every 3 days.

Cell morphology and attachment

HDFs and HUVECs were cultured on PLLA and gelatin electrospun nanofibrous membranes and were photographed by SEM 3 days after seeding. Briefly, membranes were harvested, washed with PBS three times and fixed with 4% glutaraldehyde for 2 hours at 4°C. Next, after a standard ethanol series followed by three rinsing steps with distilled water, the samples were dehydrated. Dry specimens were sputter coated with

gold and the cell morphologies on the fibrous membranes were observed by SEM.

To analyze the cells adhesion on the fibrous membranes, HDFs and HUVECs adhering on the membranes were stained with 4, 6-diamidino-2-phenylindle (DAPI) and counted after 12 hours and 3 days of incubation, respectively. The culture medium was removed and cell-membrane samples were washed three times with PBS and then fixed with 4% neutral formalin for 10 minutes after being treated with DAPI for 5 min for nuclei staining. Nuclei fluorescent images were acquired using a fluorescence microscope and the cell density was estimated by selecting 4 different randomly chosen areas per membrane at 100 × magnification where the number of cells was counted. The average cells number in 4 spots was considered the value of cell density. All counts were performed by three investigators blinded to the samples.

Cell viability detection

Cell viability was analyzed by a CCK-8 assay on 1, 3 and 5 days after seeding. Briefly, the culture medium was removed and cell-membrane samples were washed three times with PBS, and then the samples were transferred to another 12-well culture plate with 1000 μL of culture medium in each well. After incubation at 37°C for 1 hour, 100 μL of CCK-8 reagent was added to each sample and the samples were incubated at 37°C for 2 hour according to the reagent instruction. 100 μL of incubated medium was transferred to a 96 -well culture plate to measure the absorbance intensity of each sample at a wavelength of 450 nm by a microplate reader (Thermo Lab-systems, USA). All experiments were performed in triplicate.

Rat model of random skin flap

Thirty healthy male Sprague Dawley rats aged 4-5 weeks and weighing 75-110 g were obtained from SLAC National Rodent Laboratory Animal Resources (Shanghai, China) and used in this study. The Committee of Experimental Animal Administration of Shanghai Ninth People's Hospital Affiliated Shanghai Jiao Tong University School of Medicine approved all the animal study protocols, and this study was performed in accordance with the international ethics guidelines and the National Institutes of Health Guide concerning the Care and Use of Laboratory Animals. Rats were maintained under specific pathogen-free conditions (SPF).

The random skin flap model was used as previously described.[19,20] Briefly, the animals were anesthetized and operated under sterile conditions. A random pattern, caudally-based dorsal flap (1.5×5.0 cm) was performed in the dorsum of the rats. The flap without axial vessels was then incised with scalpel, being elevated in a plane superficial to the deep muscular fascia. Therefore, the ischemic gradient was proportional to the distance from the base. Rats were randomly divided into three groups (n=10): group A (no-treatment group, Control); group B (PLLA membrane group, PLLA); group C (gelatin membrane group, Gel). The flaps in groups B and C were implanted with the corresponding membranes to the underlying bed, and the flap was sutured in place. After recovery from anesthesia, the rats were returned to their cages.

Macroscopic evaluation and skin blood perfusion

On day 7 post-operation, the flaps survival and necrotic areas were recorded using a digital camera. The flaps survival and necrosis were assessed by gross appearance, color, presence or absence of bleeding cuts and flaps consistency, with the total flap area

defined by the surgical borders. The necrotic area was divided by the total flap area, and the results were expressed as skin necrosis percentages. The surface area of these defined zones was measured using Image-Pro Plus version 6.0 Software (version 6.0; Media Cybernetics LP, Silver Spring, MD, USA).

Blood perfusion of the skin flap was measured with a laser Doppler flowmetry (Moor Instruments, Axminster, UK) on day 7 post-operation. The low-resolution/high-speed images were set for time constant of 1.0 s, a display rate of 25 Hz, and camera exposure time of 20 ms. Results were recorded as blood perfusion units (PU).

Histological Analysis

On day 7 post-operation, tissue sections from same positions of the flaps were harvested. These specimens were fixed with 4% neutral formalin for 24 h, embedded in paraffin, cross-sectioned along the tissue, and stained using hematoxylin–eosin (H&E) and Masson's trichrome for light microscopy.

Microvessel density (MVD) and inflammatory response detection

Consecutive specimens (5 μm apart) were obtained from the paraffin embedded tissues for immunohistochemical analysis of CD31and CD68. Briefly, after deparaffinization, endogenous peroxidase activity was quenched with 3% H_2O_2 for 10 min, and then a heat based antigen retrieval step was performed. Subsequently, the tissue was blocked with 5% BSA and treated with primary antibody against CD31 (Abcam, US) and CD68 (Abcam, US) at 4°C overnight. The next day, the sections were incubated with a HRP conjugated goat antibody used as the secondary. Sections were then observed and photographed with the microscope (Nikon, Japan) connected to a

digital camera.

To assess MVD, three high staining areas per section were chosen under a low magnification (×100) for each group. Then, the microvessel numbers were counted within the hot spot area at 200× magnification. Only the vessel with a clearly defined lumen was considered a countable microvessel, while the indistinguishable vessels were not counted. The MVD value was defined as the average vessel count in 3 hot spots. All counts were performed by three investigators blinded to the samples.

To evaluate the macrophage infiltration, the CD68+ cell density was valued by selecting 5 different and random areas per section at 200× magnification and the number of cells was counted. The average number of cells in 5 spots was considered the cell density value. All counts were performed by three investigators blinded to the samples.

Statistical Analysis

The data were analyzed by ANOVA with a post hoc Dunn or Bonferroni examination. All the data were processed by IBM SPSS Statistics 19 for Windows. A value of $p < 0.05$ was considered statistically significant.

Results

Characterization of electrospun fibrous membranes

As shown in Figure 1, the surface of both the PLLA and gelatin fibers showed a uniform shape and stable fiber structure. The PLLA fibers diameter was 1.31 ± 0.27 μm (Fig. 1a), while the gelatin fibers diameter was 1.21 ± 0.19 μm (Fig. 1b). There difference between the two values was not statistically significant. According to the

strain/stress curves (Fig. 1c), the PLLA membrane tensile strength was 1.38 ± 0.29 MPa, and the tensile modulus was 29.8 ± 3.4 MPa, while the gelatin fiber tensile strength and tensile modulus was 0.68 ± 0.13 MPa and 3.8 ± 0.35 MPa, respectively. The gelatin fibers showed lower tensile strength and elongation at break compared to the PLLA fibers.[21,22] The electrospun fibrous membranes static WCAs were measured to determine the electrospun fibers surface properties. The WCAs were 133 ± 3° and 0° for PLLA and gelatin electrospun fibers (Fig. 1d), respectively. The results showed that natural gelatin fibers exhibited significantly improved hydrophilicity compared with the synthetic PLLA fibers ($p < 0.05$).

Cell attachment and viability on different electrospun fibrous membranes

The cell morphology of HDFs and HUVECs grown on electrospun PLLA and gelatin membranes was observed by SEM on day 3 (Fig. 2). Both HDFs and HUVECs were firmly and better attach to the gelatin membranes, acquiring a spherical morphology and forming plenty of filiform pseudopodia linked to the fibers. However, the HDFs on electrospun PLLA membranes showed spindle or fiber-like morphology after 3 days of culture, while the HUVECs exhibited a flattened morphology on the electrospun PLLA membranes.

To determine the number of HDFs and HUVECs adhered to and grown on the surface of the two different membranes, DAPI was used to stain the nuclei. As Figure 3A shown, after 12 hour of culturing, more cells were adhered to the electrospun gelatin membranes than those on the electrospun PLLA membranes ($p < 0.05$), but the result was not statistically different. After 3 days of culture, the same trend was observed (Fig. 3A).

The CCK-8 assay was consistent with the fluorescent observations. Indeed, more cells growth on the surface of the electrospun gelatin membranes was found at day 3. Figure 3B shows a similar growth behavior of HDFs and HUVECs cultured on the two different electrospun fibrous membranes within 3 days. Indeed, for both HDFs and HUVECs, viability on the PLLA scaffolds was the lowest after 12 hours and 3 days of culture. Because of the poor hydrophilicity of the electrospun PLLA fibers, cell adhesion and growth was poor, thus the cells showed a lower viability compared with the cells growing on the gelatin membranes ($p < 0.05$). These results indicated that the hydrophilic electrospun gelatin membranes allowed a better cell adhesion and growth.

Influence of different eletrospun fibrous membranes on flap viability

The random skin flaps were treated with different eletrospun fibrous membranes and their necrotic area was analyzed on day 7 post-operation. The necrosis ratio was calculated as the necrotic skin area/the whole skin flap area in each sample. It was observed that the necrotic skin regions were clearly distinguishable from the surviving flap. The necrotic skin without adequate blood flow became black and rigid. On day 7 post-operation, the necrosis ratio of the control and PLLA groups was 49 ± 2% and 54 ± 3% respectively, although the difference was not statistically. Less skin flap necrosis was observed in the gelatin group on day 7, with a necrosis ratio of 29 ± 5% ($p < 0.05$).

To analyze whether different eletrospun membrane materials would influence the blood supply of the skin flap, blood perfusion of skin flap was tested (Fig. 4). According to the color laser Doppler imaging system analysis, the blood perfusion units in the control and PLLA were 442 ± 28 and 319 ± 50 respectively, with no statistically significant difference. The blood perfusion units in the gelatin group (623 ± 44) was

significantly higher than the control and PLLA group, indicating that the eletrospun gelatin membranes played an important role in promoting blood perfusion ($p < 0.05$).

As Figure 5A b and c shown, the two kinds of eletrospun fibrous membranes were not fully biodegraded after 7 days post-operation, especially the eletrospun PLLA membranes, still showing a relatively complete structure. On the other hand, Figure 5B d and e show that the collagen fibers were denser around the eletrospun PLLA membranes compared to the gelatin membranes.

Influence of different eletrospun fibrous membranes on ischemic skin flaps neovascularization

To assess the impact of different eletrospun fibrous membranes on ischemic skin flaps neovascularization, we examined the microvessels distribution in the skin flaps by CD31 immunohistochemical staining. As Figure 6A shows, the flap treated with the gelatin membrane possessed more capillary vessels with a dilated lumen compared with the control and PLLA groups. Moreover, a higher number of CD31-positive cells in gelatin membrane-treated flaps was found.

MVD was investigated by counting the CD31 positive microvessels number per hot spots in each section (Fig. 6B). Compared with the control (35 ± 3) and PLLA (28 ± 3) group, MVD value in the gelatin group (53 ± 6) was clearly higher 7 days after operation ($p<0.05$).

The inflammatory response caused by different eletrospun fibrous membranes

To study the inflammatory response caused by the different materials, inflammatory cell infiltration into the implants was evaluated in each section using an anti-CD68

(macrophages) immunohistochemical staining 7 days after implantation. Both the transplanted membranes groups contained more CD 68 positive cells compared with the staining in the control group (22 ± 2 cells /HFP). Furthermore, significantly more CD68+ cells were observed in the PLLA group (118 ± 8 cells/HFP) than in the gelatin group (51 ± 7 cells/HFP) ($p < 0.05$; Fig. 6C)

Discussion

Despite plenty of efforts have been spent to improve the survival rate of random skin flap and achieved good results, there is continual effort to improve the survival rate of random skin flaps.[23,24] Electrospun fibrous membrane with a high surface area and porous structure can mimic the natural extracellular matrix (ECM) as the substrate for tissue repair, and at the same time promote the nutrients exchange.[25,26] The aforementioned characteristics made it widely used in skin regeneration. For instance, we previously fabricated bFGF-loaded hydrophilic electrospun PLGA scaffolds by surface modification to promote wound healing and skin regeneration.[27] Yao et al prepared electrospun gelatin nanofibers containing centella asiatica which exhibited dermal wound-healing activity in a rat model.[28] Thus, the electrospinning fibrous membrane has the potential for application as a therapy for improving skin flap survival.

In the present study, we investigated electrospinning fibrous membrane prepared with natural (gelatin) and synthetic (PLLA) materials for application in the random skin flap. Our results showed that the gelatin fibrous membrane possessed better biocompatibility. After implantation into the skin flap of the rat model, the gelatin fibrous membrane showed weaker foreign body reaction and did not cause strong inflammation.

Furthermore, the gelatin fibrous membrane was beneficial to the formation of vasculature. Thereby, the gelatin membrane was a better choice for random skin flap survival compared to the PLLA membrane.

For dermal cell culture, the tensile strength of electrospun fibrous membranes ranging from 0.8 to 18.0 MPa was adequately durable.[29] In addition, fibrous membranes were not designed to permanently replace native tissue, and the characteristic of the membranes do not need to be exactly the same with that of the host environment. The membrane simply needs to be independent and be adapted to the mechanical strength of the implant site itself and be appropriated for cell growth. Thus, the implant membrane can serve as temporary constructs for the release of loaded drugs and growth factors or implanted and native cells to ultimately proliferate and regenerate the tissue. Moreover, as the cells migrate into the fibrous membrane, the consolidated membrane provides a better mechanical support.

Porosity and wettability are the characteristics of ideal membranes for cell culture purposes, which should allow cell infiltration and efficient nutrients exchange.[30,31] Compared with the PLLA fibrous membrane, the gelatin fiber showed higher hydrophilicity, allowing a better cell adhesion.

Dermal fibroblasts can secrete a large number of growth factors, such as bFGF and VEGF, which plays a critical role in neovascularization.[32] In addition, endothelial cells are important in the vascular tissue.[33] Many tissue-engineered blood vessels are made from dermal fibroblasts and endothelial cells.[34] Hence, we investigated the HDF and HUVEC adhesion and viability on two kinds of electrospinning fibrous membrane *in vitro*. In the present study, HDFs and HUVECs on the surface of porous membranes showed a spherical morphology with plenty of filiform pseudopodia, gathering in the

membranes pores. The reason may be that, compared to the PLLA fiber, porous gelatin electrospun fiber has a stronger water imbibition with stronger ability for protein adsorption from the cell culture medium to improve cell adhesion, such as integrin and fibronectin, and thus a strong adhesion prevented the detrimental separation of the cell tail and fiber during the process of cell migration, which is not conductive to cells stretch on the gelatin fibers. Consequently, the cells on the gelatin membranes showed a spherical morphology.[35] The gelatin fibers nature allowed a long-term cell proliferation by reducing the contact inhibition effect after cell stretching and being connected to other cells. On the other hand, the HDFs did not completely spread and still kept the spindle morphology on the PLLA fibrous membrane after 3 days of culture. HUVECs also showed a flat shape on the PLLA membrane. The DAPI staining showed that, both HUVECs and HDFs number on the gelatin membrane was much more than that on the PLLA membrane at 12 hours and 3 days. Additionally, the CCK-8 assay results (Fig. 5) suggested that HDF and HUVEC growth behavior was better on the gelatin membrane compared with the PLLA membrane.

Degradation is one of characteristics of tissue engineering material, and reparation of different tissues requires biomaterials with different degradation time.[36,37] Thus, the biomaterials with a degradation rate in line with the tissue repair process are more suitable to tissue repair. In our study, H&E staining showed that PLLA membrane degradation was slower than gelatin membrane degradation after 7 days of implantation. Moreover, fibrosis caused by relatively intact PLLA membrane was more severe than gelatin membrane as Fig. B shown. Therefore, the gelatin membrane did not show fibrosis wrap at 7 days of implant, thus allowing it to exert its role of biological scaffold for tissue repair. Hence, the degradation rate of gelatin electrospun nanofibers was more

suitable for skin flap repair compared to PLLA electrospun nanofibers.

It is well known that prolonged or excess inflammation can lead to flap tissue damage in a persistently inflamed state due to ischaemia and reperfusion injury.[38,39] PLLA has been widely used as the potential ideal tissue engineering material. However, because the PLLA degradation product is lactic acid, acidic degradation product can cause a strong inflammatory response after PLLA degrades. Moreover, synthetic polymer implanted into flap might cause a foreign body reaction, which might recruit more inflammatory cells. Furthermore, PLLA that cannot degrade in a relatively short period might aggravate the inflammatory reaction. Our results showed the presence of inflammatory cell infiltration after the membrane was implanted. Less CD68+ cells were present in the implanted electrospun gelatin nanofibers membrane after 7 days implantation. This result indicated that the gelatin nanofibers membrane had better biocompatibility. On the other hand, inflammation cells secrete a certain amount of growth factors, such as VEGF, bFGF and PDGF, which can promote the formation of new blood vessels, to promote the survival of skin flap. In our study, the CD31 positive cells results showed more microvascular formation after gelatin fibrous membrane implantation, which was potentially beneficial for the flap tissue.

Electrospun fibrous membrane has already been widely used in many kinds of tissue repair, such as skin wound, tendon injury and hernia.[40-42] However, we are the first investigating the feasibility of electrospun nanofibers membranes made of synthetic and natural materials in the random skin flap survival. Our results showed that natural materials were more suitable for application in the random skin flap, since it was more beneficial to revascularization compared to the synthetic materials. However, we also realized that the gelatin electrospinning fibrous membrane preparation process by

glutaraldehyde crosslinking was complicated, and glutaraldehyde may injure the cells. In addition, the gelatin electrospinning fibrous membrane could not completely degrade after 7 days implantation, which was not consistent with the skin flap repair time. Therefore, further research should focus on the improvement the material preparation process, acceleration of the material degradation and incorporation of drugs, growth factors and cells into the material to improve random skin flap survival.

Conclusion

The results in the present work indicated that 2D gelatin electrospun nanofibrous membranes possessed a better hydrophilicity with a stable fibrous structure. During *in vitro* culture, HDFs and HUVECs adhered better to the gelatin fiber than to the PLLA fibers and showed a better vitality in the gelatin fiber. In a rat model, after 7 days of implantation, blood perfusion of the flap treated with gelatin membrane was higher than other groups. From histology tests, in comparison to PLLA, gelatin did not cause severe inflammation reaction and allowed the formation of new blood vessels. Therefore, electrospun fibrous membranes prepared with natural materials such as gelatin might have potential advantages in the promotion skin flap survival rate.

Acknowledgements

This work was supported in part by National Natural Science Foundation of China (81372073 and 51373112), Jiangsu Provincial Special Program of Medical Science (BL2012004), Jiangsu Provincial Clinical Orthopedic Center, the Priority Academic Program Development of Jiangsu Higher Education Institutions (PAPD).

References

1. L. Borbély and A. Kovács, *Acta Chir. Hung.*, 1986, **27**, 185-194.
2. Y. Demirtas, S. Ayhan, Y. Sariguney, F. Findikcioglu, O. Cukurluoglu, O. Latifoglu and S. Cenetoglu, *Plast. Reconstr. Surg.*, 2006, **117**, 272-276.
3. V. Valentini, A. Cassoni, T. M. Marianetti, V. Mitro, P. Gennaro, C. Ialongo and G. Iannetti, *J. Craniofac. Surg.*, 2008, **19**, 1080-1084.
4. J. Nolan, R. A. Jenkins, K. Kurihara and R. C. Schultz, *Plast. Reconstr. Surg.*, 1985, **75**, 544-551.
5. B. H. Haughey and W. R. Panje, *Arch Otolaryngol*, 1985, **111**, 234-240.
6. C. E. Attinger, C. A. Picken, T. R. Troost and R.B. Sessions, *Otolaryngol Head Neck Surg.*, 1996, **114**, 148-157.
7. A. Ozturk, C. Fırat, H. Parlakpınar, A. Bay-Karabulut, H. Kirimlioglu and A. Gurlek, *Exp. Diabetes Res.*, 2012, 2012:721256.
8. C. Y. Huang and Z. Y. Shen, *Zhongguo Xiu Fu Chong Jian Wai Ke Za Zhi*, 2003, **17**, 293-297.
9. Y. Zheng, C. Yi, W. Xia, T. Ding, Z. Zhou, Y. Han and S. Guo. *Plast. Reconstr. Surg.*, 2008, **121**, 59-69.
10. H. L. Prichard, W. M. Reichert and B. Klitzman, *Biomaterials*, 2007, **28**, 936-946.
11. C. J. Bettinger, *Macromol Biosci.*, 2011, **11**, 467-482.
12. X. Sun, L. Cheng, W. Zhu, C. Hu, R. Jin, B. Sun, Y. Shi, Y. Zhang and W. Cui, *Colloids Surf. B Biointerfaces*, 2014, **115**, 61-70.
13. B. Liu, S. Zhang, X. Wang, J. Yu and B. Ding, *J. Colloid Interface Sci.*, 2015, **457**, 203-211.

14. Y. B. Truong, V. Glattauer, K. L. Briggs, S. Zappe and J. A. Ramshaw, *Biomaterials*, 2012, **33**, 9198-9204.
15. K. Siimon, H. Siimon and M. Järvekülg, *J. Mater. Sci. Mater. Med.*, 2015, **26**, 5375.
16. L. Zhou, C. H. Zhu, L. Edmonds, H. L. Yang, W. G. Cui and B. Li, *RSC Advances*, 2014, **4**, 43220-43226.
17. X. Zhao, S. Jiang, S. Liu, S. Chen, Z. Y. Lin, G. Pan, F. He, F. Li, C. Fan and W. Cui, *Biomaterials*, 2015, **61**, 61-74.
18. W. Cui, X. Li, X. Zhu, G. Yu, S. Zhou and J. Weng, *Biomacromolecules*, 2006, **7**, 1623-1629.
19. I. Serdaroglu, K. Islamoglu and E. Ozgentas, *J. Reconstr. Microsurg.*, 2005, **21**, 51-56.
20. D. Bagdas, B. Cam Etoz, S. Inan Ozturkoglu, N. Cinkilic, M. O. Ozyigit, Z. Gul, N. Isbil Buyukcoskun, K. Ozluk and M. S. Gurun, *Biol. Pharm. Bull.*, 2014, **37**, 361-370.
21. C. E. Ayres, G. L. Bowlin, R. Pizinger, L.T. Taylor, C. A. Keen, D. G. Simpson, *Acta Biomater.*, 2007, **3**, 651-61.
22. W. G. Cui, L. Y. Cheng, H. Y. Li, Y. Zhou, Y. G. Zhang, J. Chang, *Polymer*, 2012, **53**, 2298-2305.
23. L. S. Nichter, M. W. Sobieski and M. T. Edgerton, *Plast. Reconstr. Surg.*, 1985, **75**, 847-852.
24. C. Wang, Y. Cai, Y. Zhang, Z. Xiong, G. Li and L. Cui, *PLoS One*, 2014, **9**, e100818.
25. J. Pelipenko, P. Kocbek, B. Govedarica, R. Rošic, S. Baumgartner and J. Kristl, *Eur J. Pharm. Biopharm.*, 2013, **84**, 401-411.
26. C. Hu, S. Liu, Y. Zhang, B. Li, H. Yang, C. Fan and W. Cui, *Acta Biomater.*, 2013, **9**,

7381-7388.

27. X. Sun, L. Cheng, J. Zhao, R. Jin, B. Sun, Y. Shi, L. Zhang, Y. Zhang and W. Cui, *J. Mater. Chem. B*, 2014, **2**, 3636-3645.
28. C. H. Yao, J. Y. Yeh, Y. S. Chen, M. H. Li and C. H. Huang, *J. Tissue Eng. Regen. Med.*, 2015, Feb 25.
29. W. G. Cui, X. L. Zhu, X. H. Li, and Y. Jin, *Materials Science and Engineering C*, 2009, **29**, 1869.
30. K. Park, Y. M. Ju, J. S. Son, K. D. Ahn and D. K. Han, *J. Biomater. Sci. Polym. Ed.*, 2007, **18**, 369-382.
31. X. Zhu, W. Cui, X. Li and Y. Jin, *Biomacromolecules*, 2008, **9**, 1795-1801.
32. S. Ding, C. Li, S. Lin, Y. Yang, D. Liu, Y. Han, Y. Zhang, L. Li, L. Zhou and S. Kumar, *Hum. Pathol.*, 2006, **37**, 861-866.
33. S. H. Ku and C. B. Park, *Biomaterials*, 2010, **31**, 9431-9437.
34. E. Mohammadi, S. M. Nassiri, R. Rahbarghazi, V. Siavashi and A. Araghi, *Cell Tissue Res.*, 2015, Jun 12.
35. S. P. Palecek, J. C. Loftus, M. H. Ginsberg, D. A. Lauffenburger and A. F. Horwitz, *Nature*, 1997, **385**, 537-540.
36. H. Doyle, S. Lohfeld and P. McHugh, *Med. Eng. Phys.*, 2015, **37**, 767-776.
37. S. Zhao, J. Zhao, S. Dong, X. Huangfu, B. Li, H. Yang, J. Zhao and W. Cui, *Int. J .Nanomedicine*, 2014, **9**, 2373-2385.
38. H. J. Kim, L. Xu, K. C. Chang, S. C. Shin, J. I. Chung, D. Kang, S. H. Kim, J. A. Hur, T. H. Choi, S. Kim and J. Choi, *Microsurgery*, 2012, **32**, 563-570.
39. A. Can, M. Temel, R. Dokuyucu and M. Mutaf, *Ann. Plast. Surg.*, 2015, May 7.
40. C. H. Woo, Y. C. Choi, J. S. Choi, H. Y. Lee and Y. W. Cho, *J. Biomater. Sci. Polym.*

Ed., 2015, **26**, 841-854.

41. S, Liu, M, Qin, C, Hu, F, Wu, W, Cui, T. Jin and C. Fan, *Biomaterials*, 2013, **34**, 4690-4701.
42. G. C. Ebersole, E. G. Buettmann, M. R. MacEwan, M. E. Tang, M. M. Frisella, B. D. Matthews and C. R. Deeken, *Surg. Endosc.*, 2012, **26**, 2717-2728.

Scheme 1

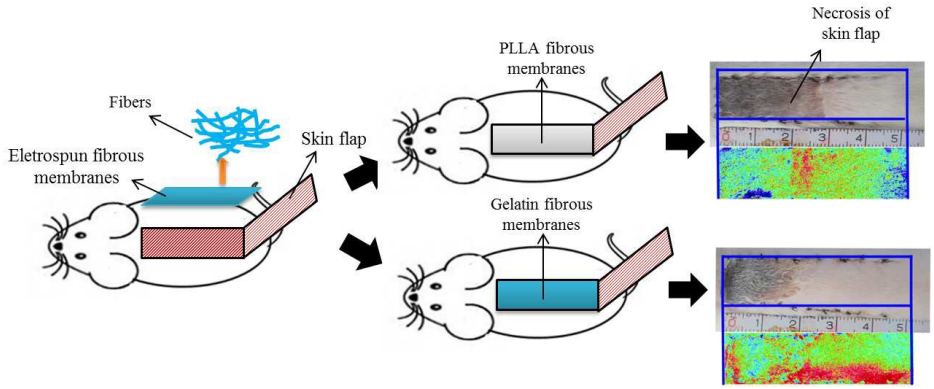

Scheme 1. Schematic workflow for implanting electrospun nanofibrous membranes under the random skin flap.

Figure 1

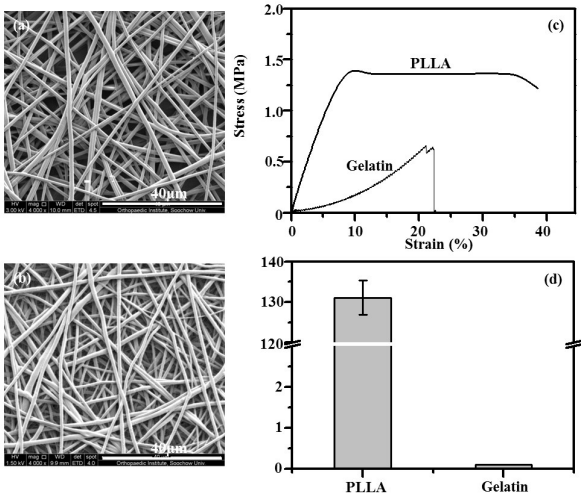

Fig. 1 The morphology of electrospun fibers of PLLA (a) and gelatin (b); stress/strain curves (c) and water contact angles (d) of electrospun fibrous membranes.

Figure 2

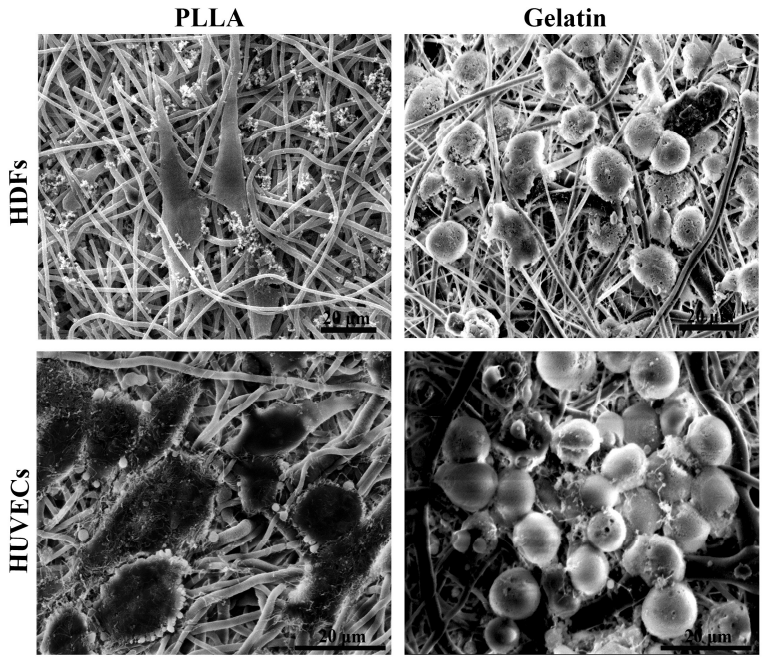

Fig. 2 SEM images of HDFs and HUVECs growth on the electrospun PLLA and gelatin fiberous membranes after 3 days of culture.

Figure 3

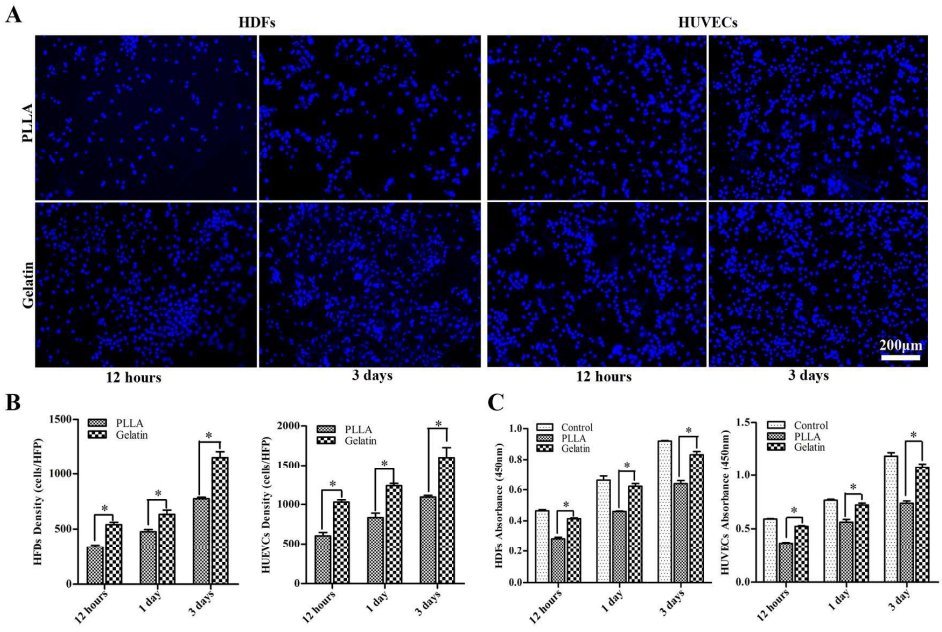

Fig. 3 HDFs and HUVECs density and viability on fibrous membranes. (A) DAPI staining of HDFs and HUVECs cultured on both the membranes at 12 hours and 3 days. (B) Cell density on both membranes at 12 hours, 1 day and 3 days after seeding. (C) CCK-8 assay of HDF and HUVEC viability after 12 hours, 1day and 3 days' culture on the TCP, PLLA, and gelatin membranes. TCP was used as control. * $p < 0.05$ compared to the corresponding controls.

Figure 4

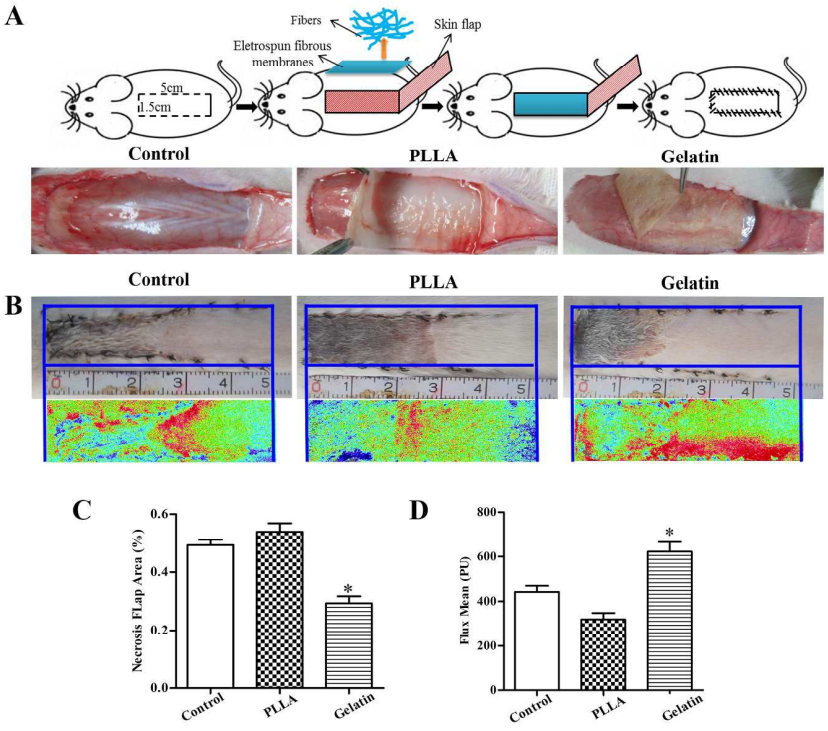

Fig. 4 Analysis of necrosis and blood flow perfusion of the skin flap after treatment. (A) Schematic workflow for implanting electrospun nanofibrous membranes under the random skin flap and photographic images of implanting electrospun nanofibrous membranes (B) Photographic images of the skin flap and color laser Doppler detection of skin flaps from the control, PLLA and gelatin groups 7 days post-operation. The color scale illustrates variations in the blood flow, from maximal (red) to minimal perfusion (dark blue). (C) The necrosis ratio in the corresponding groups on day 7 after operation. (D) Quantitative analysis of blood flow perfusion of the flap measured as mean perfusion units ± standard error. *represents $p < 0.05$ compared to the corresponding controls.

Figure 5

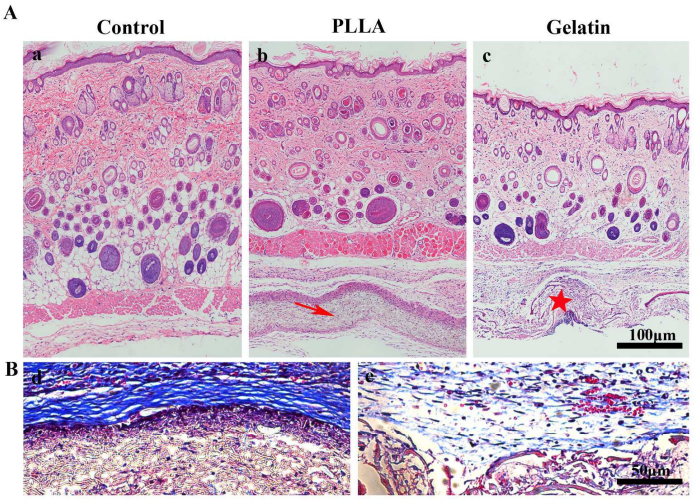

Fig. 5 Light microscope images of the skin flaps. (A) H&E stained images of all groups of skin flaps 7 days after surgery. Control group (a), PLLA group (b) and Gelatin group (c). The red arrow indicated the eletrospun PLLA membranes. The red star indicated the eletrospun gelatin membranes. (B) Masson's trichrome staining of the PLLA group (d) and gelatin group (e).

Figure 6

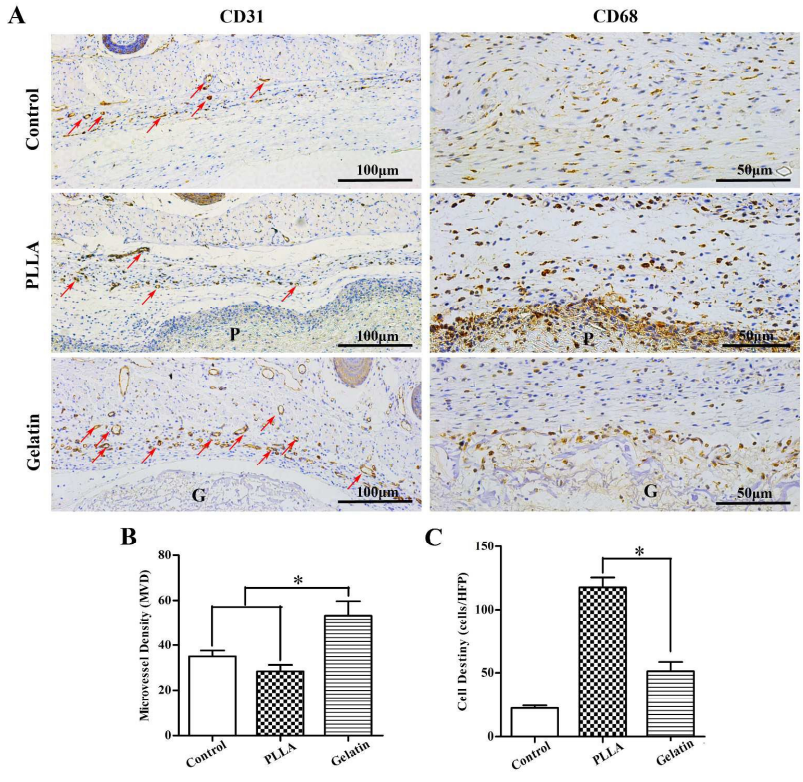

Fig. 6 Vascularization and inflammatory response. (A) Immunohistochemical analysis of CD31and CD68. (B) Microvessel density (MVD) of each group on post operation day 7. (C) CD68+ cell density of each group on post operation day 7. The red arrow indicated the capillary vessels. * represents $p < 0.05$ compared to the control.

Figure Captions

Scheme 1. Schematic workflow for implanting electrospun nanofibrous membranes under the random skin flap.

Fig. 1 The morphology of electrospun fibers of PLLA (a) and gelatin (b); stress/strain curves (c) and water contact angles (d) of electrospun fibrous membranes.

Fig. 2 SEM images of HDFs and HUVECs growth on the electrospun PLLA and gelatin fiberous membranes after 3 days of culture.

Fig. 3 HDFs and HUVECs density and viability on fibrous membranes. (A) DAPI staining of HDFs and HUVECs cultured on both the membranes at 12 hours and 3 days. (B) Cell density on both membranes at 12 hours, 1 day and 3 days after seeding. (C) CCK-8 assay of HDF and HUVEC viability after 12 hours, 1day and 3 days' culture on the TCP, PLLA, and gelatin membranes. TCP was used as control. * $p < 0.05$ compared to the corresponding controls.

Fig. 4 Analysis of necrosis and blood flow perfusion of the skin flap after treatment. (A) Schematic workflow for implanting electrospun nanofibrous membranes under the random skin flap and photographic images of implanting electrospun nanofibrous membranes (B) Photographic images of the skin flap and color laser Doppler detection of skin flaps from the control, PLLA and gelatin groups 7 days post-operation. The color scale illustrates variations in the blood flow, from maximal (red) to minimal perfusion (dark blue). (C) The necrosis ratio in the corresponding groups on day 7 after operation. (D) Quantitative analysis of blood flow perfusion of the flap measured as mean perfusion units ± standard

error. *represents $p < 0.05$ compared to the corresponding controls.

Fig. 5 Light microscope images of the skin flaps. (A) H&E stained images of all groups of skin flaps 7 days after surgery. Control group (a), PLLA group (b) and Gelatin group (c). The red arrow indicated the eletrospun PLLA membranes. The red star indicated the eletrospun gelatin membranes. (B) Masson's trichrome staining of the PLLA group (d) and gelatin group (e).

Fig. 6 Vascularization and inflammatory response. (A) Immunohistochemical analysis of CD31and CD68. (B) Microvessel density (MVD) of each group on post operation day 7. (C) CD68+ cell density of each group on post operation day 7. The red arrow indicated the capillary vessels. * represents $p < 0.05$ compared to the control.

Graphical and textual abstract

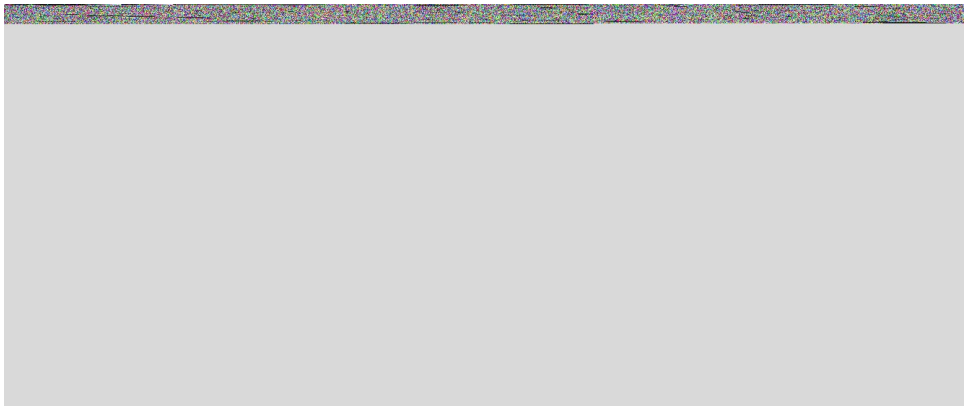

Electrospun fibrous membranes made of natural materials are more advantageous for random skin flap survival, and can be used as carrier implantation materials for improving skin flap survival rate